J. Fluid Mech. (2014), *vol.* 751, *pp.* 121–141.
doi:10.1017/jfm.2014.290

The Burnett equations in cylindrical coordinates and their solution for flow in a microtube

Narendra Singh and Amit Agrawal†

Department of Mechanical Engineering, Indian Institute of Technology Bombay, Powai, Mumbai 400076, India

(Received 13 January 2014; revised 29 April 2014; accepted 20 May 2014; first published online 16 June 2014)

The Burnett equations constitute a set of higher-order continuum equations. These equations are obtained from the Chapman–Enskog series solution of the Boltzmann equation while retaining second-order-accurate terms in the Knudsen number Kn. The set of higher-order continuum models is expected to be applicable to flows in the slip and transition regimes where the Navier–Stokes equations perform poorly. However, obtaining analytical or numerical solutions of these equations has been noted to be particularly difficult. In the first part of this work, we present the full set of Burnett equations in cylindrical coordinates in three-dimensional form. The equations are reported in a generalized way for gas molecules that are assumed to be Maxwellian molecules or hard spheres. In the second part, a closed-form solution of these equations for isothermal Poiseuille flow in a microtube is derived. The solution of the equations is shown to satisfy the full Burnett equations up to $Kn \leqslant 1.3$ within an error norm of $\pm 1.0\,\%$. The mass flow rate obtained analytically is shown to compare well with available experimental and numerical results. Comparison of the stress terms in the Burnett and Navier–Stokes equations is presented. The significance of the Burnett normal stress and its role in diffusion of momentum is brought out by the analysis. An order-of-magnitude analysis of various terms in the equations is presented, based on which a reduced model of the Burnett equations is provided for flow in a microtube. The Burnett equations in full three-dimensional form in cylindrical coordinates and their solution are not previously available.

Key words: micro-/nano-fluid dynamics, non-continuum effects, rarefied gas flow

1. Introduction

The Knudsen number (Kn), defined as the ratio of the mean free path of the gas (λ) divided by the characteristic length scale, classifies flow into four regimes: continuum ($Kn \leqslant 10^{-3}$), slip ($10^{-3} < Kn \leqslant 10^{-1}$), transition ($10^{-1} < Kn \leqslant 10$) and free-molecular ($Kn > 10$). The Navier–Stokes (NS) equations are applicable in the continuum regime and possibly in the slip regime (Agrawal & Dongari 2012). However, the continuum assumption under which the NS equations are derived breaks down in the transition regime. The governing equation to be solved in the transition regime is not obvious. Solving the Boltzmann equation directly, which represents conservation of the number density of gas particles, involves huge computational cost. The nonlinear

† Email address for correspondence: amit.agrawal@iitb.ac.in

nature of this integro-partial differential equation poses further challenges. Retaining second-order-accurate terms in the Knudsen number in the Chapman–Enskog series solution of the Boltzmann equation seems pertinent to flows in the slip and transition regimes. Gas flows in rarefied regimes ($Kn \gg 0.001$) have been tackled with different higher-order continuum models, such as the Burnett, BGK (Bhatnagar–Gross–Krook) Burnett (Agarwal, Yun & Balakrishnan 2001), augmented Burnett (Zhong 1991), regularized Burnett (Jin & Slemrod 2001), super-Burnett (Agarwal *et al.* 2001), Grad's moment (Grad 1949), R13 (Struchtrup & Torrilhon 2003) or R26 (Gu & Emerson 2009) equations. These models are able to capture many rarefied phenomena such as nonlinear pressure drop in the case of microchannels (Pong *et al.* 1994; Zohar *et al.* 2002).

However, the Burnett equations apparently suffer from certain problems. For example, these equations are unstable to small-wavelength disturbances, as shown by Bobylev (1982) using linearized stability analysis. This aspect leads to challenges while solving these equations numerically. Comeaux, Chapman & MacCormack (1995) indicated that the Burnett equations can violate the second law of thermodynamics at high Knudsen numbers. García-Colín, Velasco & Uribe (2008), however, argue that these issues with the Burnett equations are actually a limitation of the existing theories (such as linear irreversible thermodynamics), and suggested the need for better theories. They further argue that some of the limitations of the Burnett equations are actually there with the NS equations as well. The BGK Burnett equations (Agarwal *et al.* 2001), derived by representing the nonlinear collision integral with the Bhatnagar–Gross–Krook model, avoids some of these issues. These equations are unconditionally stable at high Knudsen numbers and, as shown by Agarwal *et al.* (2001), satisfy the Boltzmann H-theorem. The most recent alternative form of the Burnett equations has been proposed by Dadzie (2013) without invoking the Chapman–Enskog expansion.

Although generalized three-dimensional Cartesian Burnett equations are available (for example, in Agarwal *et al.* 2001), three-dimensional cylindrical Burnett equations are not readily available owing to the complex nature of the stress and heat flux tensors. Zhong & Furumoto (1995) derived the three-dimensional cylindrical form of the augmented Burnett equations. Yang & Garimella (2009) derived the Burnett stress terms in cylindrical form. However, those are applicable only for two-dimensional isothermal flow situations. In the current paper, the authors have transformed the three-dimensional generalized form of the conventional Burnett equations from its tensor form in cylindrical coordinates for Maxwellian as well as hard-sphere (HS) molecules.

Numerical solutions of the Burnett equations have been reported by many researchers: Agarwal *et al.* (2001) for $Kn < 0.2$ for planar Poiseuille flow; Xue & Ji (2003) for $Kn < 0.18$; Bao & Lin (2008) for $Kn < 0.4$ for planar Poiseuille flow; and Uribe & Garcia (1999) for $Kn < 0.1$. The applicability of these solutions however is restricted to a small Knudsen number envelope. Similarly, the analytical solution of these equations has been limited by the underlying assumptions and the methods through which the solutions have been obtained. Analytical solutions have been derived through series expansions, asymptotic expansion and perturbation methods (Gatignol 2012; Karniadakis, Beskok & Aluru 2005; Stevanovic 2007). These solutions however are again not applicable for $Kn \geqslant 1$. Recently, Singh, Gavasane & Agrawal (2014*b*) derived an analytical solution for Couette flow for Knudsen number up to 10, using various models to establish the usefulness of the higher-order models. Singh, Dongari & Agrawal (2014*a*) solved the augmented Burnett equations for planar Poiseuille flow. Their analytical solution satisfies the full set of augmented

Burnett equations up to $Kn = 2.2$ with an error of $\pm 1\,\%$. Their solution for integral flow parameters and field properties, such as velocity profiles, also matches well with available experimental results and the direct simulation Monte Carlo (DSMC) solution.

In the current paper, the authors have extended the approach of Singh *et al.* (2014*a*) to derive an analytical solution for axisymmetric isothermal cylindrical Poiseuille flow. The solution is shown to satisfy the Burnett equations for $Kn \leqslant 1.35$. The proposed solution satisfies the conventional Burnett equations as well as the augmented and BGK Burnett equations. Comparison of the analytically obtained mass flow rate with literature values shows that the solution can be well utilized for predicting flows for $Kn \leqslant 1.3$. In addition, the contribution of the Burnett terms to the overall stress terms has been presented quantitatively. This analysis has helped in arriving at the reduced form of the Burnett equations, which is also proposed as part of this work.

2. Governing equations in cylindrical coordinates

The Boltzmann equation, upon taking moments, leads to five equations representing conservation of mass, momentum and energy. The governing equation in three-dimensional coordinates representing these laws in cylindrical coordinates can be written as follows:

$$\frac{\partial \boldsymbol{Q}}{\partial t} + \frac{1}{r}\frac{\partial r\boldsymbol{E}}{\partial r} + \frac{1}{r}\frac{\partial \boldsymbol{F}}{\partial \theta} + \frac{\partial \boldsymbol{G}}{\partial z} + \boldsymbol{S} = 0. \tag{2.1}$$

In (2.1), $\boldsymbol{E}$, $\boldsymbol{F}$ and $\boldsymbol{G}$ represent the flux vectors in r, θ and z directions, respectively; and $\boldsymbol{Q}$ can be represented as

$$\boldsymbol{Q} = \begin{pmatrix} \rho \\ \rho u \\ \rho v \\ \rho w \\ e_t \end{pmatrix}. \tag{2.2}$$

Here, ρ represents density, u, v and w represent velocity in r, θ and z directions, respectively, and e_t denotes total energy. The $\boldsymbol{E}$, $\boldsymbol{F}$ and $\boldsymbol{G}$ flux terms can be written as the summation of inviscid ($\boldsymbol{E}_I$, $\boldsymbol{F}_I$ and $\boldsymbol{G}_I$) and viscous ($\boldsymbol{E}_V$, $\boldsymbol{F}_V$ and $\boldsymbol{G}_V$) flux terms in the following way:

$$\boldsymbol{E} = \boldsymbol{E}_I + \boldsymbol{E}_V, \quad \boldsymbol{F} = \boldsymbol{F}_I + \boldsymbol{F}_V, \quad \boldsymbol{G} = \boldsymbol{G}_I + \boldsymbol{G}_V, \tag{2.3a–c}$$

where

$$\boldsymbol{E}_I = \begin{pmatrix} \rho u \\ \rho uu + p \\ \rho vu \\ \rho wu \\ (e_t + p)u \end{pmatrix}, \quad \boldsymbol{E}_V = \begin{pmatrix} 0 \\ \sigma_{rr} \\ \sigma_{\theta r} \\ \sigma_{zr} \\ u\sigma_{zr} + v\sigma_{\theta r} + w\sigma_{rr} - q_r \end{pmatrix}, \tag{2.4a,b}$$

$$\boldsymbol{F}_I = \begin{pmatrix} \rho v \\ \rho uv \\ \rho vv + p \\ \rho wv \\ (e_t + p)v \end{pmatrix}, \quad \boldsymbol{F}_V = \begin{pmatrix} 0 \\ \sigma_{r\theta} \\ \sigma_{\theta\theta} \\ \sigma_{z\theta} \\ u\sigma_{r\theta} + v\sigma_{\theta\theta} + w\sigma_{z\theta} - q_\theta \end{pmatrix}, \tag{2.5a,b}$$

$$\boldsymbol{G}_I = \begin{pmatrix} \rho w \\ \rho uw \\ \rho vw \\ \rho ww + p \\ (e_t + p)w \end{pmatrix}, \quad \boldsymbol{G}_V = \begin{pmatrix} 0 \\ \sigma_{rz} \\ \sigma_{\theta z} \\ \sigma_{zz} \\ u\sigma_{rz} + v\sigma_{\theta z} + w\sigma_{zz} - q_z \end{pmatrix}, \tag{2.6a,b}$$

and

$$e_t = \rho(c_v T + \tfrac{1}{2}\boldsymbol{u}\cdot\boldsymbol{u}). \tag{2.7}$$

In (2.1), $\boldsymbol{S}$ is a source term given as

$$\boldsymbol{S} = \begin{pmatrix} 0 \\ (\rho vv + \sigma_{\theta\theta})/r \\ (\rho vu - \sigma_{\theta r})/r \\ 0 \\ 0 \end{pmatrix}, \tag{2.8}$$

where p denotes pressure, c_v is the specific heat at constant volume, T is temperature and $\boldsymbol{u}$ denotes the velocity vector.

Constitutive relations for stress and heat flux tensors can be obtained as an approximate solution of the Boltzmann equation using the Chapman–Enskog expansion. The expressions for these constitutive relations for gas flow near thermodynamic equilibrium can be written in the following manner (with superscripts denoting Euler (*Eu*), Navier–Stokes (*NS*), Burnett (*B*) and super-Burnett (*SB*)):

$$\sigma_{ij} = \sigma_{ij}^{(Eu)} + \sigma_{ij}^{(NS)} + \sigma_{ij}^{(B)} + \sigma_{ij}^{(SB)} + O(Kn^{n+1}), \tag{2.9}$$

$$q_i = q_i^{(Eu)} + q_i^{(NS)} + q_i^{(B)} + q_i^{(SB)} + O(Kn^{n+1}), \tag{2.10}$$

where n represents the accuracy in terms of $O(Kn)$ and

$$Kn = \frac{\lambda}{L}. \tag{2.11}$$

The mean free path λ is defined as

$$\lambda = \frac{16\mu}{5\rho\sqrt{2\pi RT}}, \tag{2.12}$$

where R and μ are gas constant and viscosity, respectively.

The stress and heat flux terms obtained with $Kn \approx 0$ form the constitutive relations for the Euler equations. These zeroth-order ($n = 0$) terms are as follows:

$$\sigma_{ij}^{(Eu)} = 0, \tag{2.13}$$

$$q_i^{(Eu)} = 0. \tag{2.14}$$

Increase in the Knudsen number requires contributions from more terms in the series in (2.9) and (2.10), resulting in the conventional NS equations. When $Kn \leqslant 0.1$, the stress and heat flux terms take the following shape ($n = 1$):

$$\sigma_{rr}^{NS} = -\mu\left(\delta_1\frac{\partial u}{\partial r} + \delta_2\frac{1}{r}\frac{\partial v}{\partial\theta} + \delta_2\frac{\partial w}{\partial z} + \delta_2\frac{v}{r}\right), \tag{2.15}$$

$$\sigma_{\theta\theta}^{NS} = -\mu\left(\delta_2\frac{\partial u}{\partial r} + \delta_1\frac{1}{r}\frac{\partial v}{\partial\theta} + \delta_2\frac{\partial w}{\partial z} + \delta_1\frac{u}{r}\right), \tag{2.16}$$

$$\sigma_{zz}^{NS} = -\mu\left(\delta_2\frac{\partial u}{\partial r} + \delta_2\frac{1}{r}\frac{\partial v}{\partial \theta} + \delta_1\frac{\partial w}{\partial z} + \delta_2\frac{u}{r}\right), \tag{2.17}$$

$$\sigma_{r\theta}^{NS} = \sigma_{\theta r}^{NS} = -\mu\left(\frac{\partial v}{\partial r} - \frac{v}{r} + \frac{1}{r}\frac{\partial u}{\partial \theta}\right), \tag{2.18}$$

$$\sigma_{\theta z}^{NS} = \sigma_{z\theta}^{NS} = -\mu\left(\frac{1}{r}\frac{\partial w}{\partial \theta} + \frac{\partial v}{\partial z}\right), \tag{2.19}$$

$$\sigma_{zr}^{NS} = \sigma_{zr}^{NS} = -\mu\left(\frac{\partial u}{\partial z} + \frac{\partial w}{\partial r}\right), \tag{2.20}$$

$$q_r^{NS} = -k\frac{\partial T}{\partial r}, \tag{2.21}$$

$$q_\theta^{NS} = -k\frac{1}{r}\frac{\partial T}{\partial \theta}, \tag{2.22}$$

$$q_z^{NS} = -k\frac{\partial T}{\partial z}, \tag{2.23}$$

where k is the thermal conductivity, $\delta_1 = 1/3$ and $\delta_2 = 2/3$.

When $O(Kn) \geqslant 0.1$, the constitutive relationships become nonlinear. We present the second-order-accurate stress and heat flux terms for Burnett equations in cylindrical form ($n = 2$):

$$\begin{aligned}
\sigma_{rr}^{B} = \frac{\mu^2}{p}\Bigg[& -\left(\frac{2\omega_1}{3} - \frac{14\omega_2}{9} + \frac{2\omega_6}{9}\right)\left(\frac{\partial u}{\partial r}\right)^2 + \left(\frac{\omega_1}{3} + \frac{2\omega_2}{9} - \frac{2\omega_6}{9}\right)\left(u\frac{\partial u}{\partial r}\right) \\
& + \left(\frac{\omega_2}{3} + \frac{\omega_6}{12}\right)\left(\frac{1}{r^2}\right)\left(\frac{\partial u}{\partial \theta}\right)^2 - \left(\frac{2\omega_2}{3} + \frac{\omega_6}{6}\right)\left(\frac{v}{r^2}\frac{\partial u}{\partial \theta}\right)\left(\frac{u}{r}\right)^2 \\
& + \left(\frac{\omega_2}{3} + \frac{\omega_6}{12}\right)\left(\frac{\partial u}{\partial z}\right)^2 + \left(-\frac{\omega_1}{3} + \frac{7\omega_2}{9} - \frac{\omega_6}{9}\right)\left(\frac{u}{r}\right)^2 - \left(\frac{2\omega_2}{3} - \frac{\omega_6}{12}\right)\left(\frac{\partial v}{\partial r}\right)^2 \\
& - \left(\frac{\omega_1}{3} - \frac{7\omega_2}{9} + \frac{\omega_6}{9}\right)\left(\frac{1}{r}\frac{\partial v}{\partial \theta}\right)^2 + \left(\frac{\omega_2}{3} - \frac{\omega_6}{6}\right)\left(\frac{\partial v}{\partial z}\right)^2 + \left(\frac{2\omega_2}{3} - \frac{\omega_6}{6}\right)\left(\frac{v}{r}\frac{\partial v}{\partial r}\right) \\
& - \left(\frac{2\omega_1}{3} - \frac{14\omega_2}{9} + \frac{2\omega_6}{9}\right)\left(\frac{u}{r^2}\frac{\partial v}{\partial \theta}\right) + \left(\frac{\omega_2}{3} + \frac{\omega_6}{12}\right)\left(\frac{v}{r}\right)^2 + \left(\frac{\omega_2}{3} - \frac{\omega_6}{6}\right)\left(\frac{1}{r}\frac{\partial w}{\partial \theta}\right)^2 \\
& - \left(\frac{\omega_1}{3} - \frac{7\omega_2}{9} + \frac{\omega_6}{9}\right)\left(\frac{\partial w}{\partial z}\right)^2 - \left(\frac{2\omega_1}{3} + \frac{4\omega_2}{9} - \frac{4\omega_6}{9}\right)\left(\frac{\partial w}{\partial z}\frac{u}{r}\right) \\
& + \left(\frac{\omega_1}{3} + \frac{2\omega_2}{9} - \frac{2\omega_6}{9}\right)\left(\frac{\partial u}{\partial r}\frac{\partial w}{\partial z}\right) - \left(\frac{2\omega_2}{3} - \frac{\omega_6}{6}\right)\left(\frac{1}{r}\frac{\partial u}{\partial \theta}\frac{\partial v}{\partial r}\right) \\
& - \left(\frac{2\omega_1}{3} + \frac{4\omega_2}{9} - \frac{4\omega_6}{9}\right)\left(\frac{1}{r}\frac{\partial v}{\partial \theta}\frac{\partial w}{\partial z}\right) + \left(\frac{\omega_1}{3} + \frac{2\omega_2}{9} - \frac{2\omega_6}{9}\right)\left(\frac{1}{r}\frac{\partial u}{\partial r}\frac{\partial v}{\partial \theta}\right) \\
& - \left(\frac{2\omega_2}{3} - \frac{\omega_6}{6}\right)\left(\frac{\partial w}{\partial r}\frac{\partial u}{\partial z}\right) - \left(\frac{2\omega_2}{3} - \frac{\omega_6}{12}\right)\left(\frac{\partial w}{\partial r}\right)^2 + \left(\frac{4\omega_2}{3} - \frac{\omega_6}{3}\right)\left(\frac{1}{r}\frac{\partial w}{\partial \theta}\frac{\partial v}{\partial z}\right) \\
& - \frac{\omega_3}{3}\frac{R}{r}\frac{\partial T}{\partial r} + \frac{2\omega_3 R}{3}\frac{\partial^2 T}{\partial r^2} - \frac{\omega_3 R}{3}\frac{\partial^2 T}{\partial z^2} - \frac{\omega_3}{3}\frac{R}{r^2}\frac{\partial^2 T}{\partial \theta^2} + \frac{2\omega_4}{3}\frac{R}{p}\frac{\partial T}{\partial r}\frac{\partial p}{\partial r} \\
& - \frac{\omega_4}{3}\frac{R}{p}\frac{\partial T}{\partial z}\frac{\partial p}{\partial z} - \frac{\omega_4}{3}\frac{1}{r^2}\frac{R}{p}\frac{\partial T}{\partial \theta}\frac{\partial p}{\partial \theta} + \frac{2\omega_5}{3}\frac{R}{T}\left(\frac{\partial T}{\partial r}\right)^2 - \frac{\omega_5}{3}\frac{R}{T}\left(\frac{\partial T}{\partial z}\right)^2
\end{aligned}$$

$$-\frac{\omega_5}{3}\frac{1}{r^2}\frac{R}{T}\left(\frac{\partial T}{\partial\theta}\right)^2-\frac{2\omega_2}{3}\frac{1}{\rho}\frac{\partial^2 p}{\partial r^2}+\frac{\omega_2}{3}\frac{1}{\rho}\frac{\partial^2 p}{\partial z^2}+\frac{\omega_2}{3}\frac{1}{r^2}\frac{1}{\rho}\frac{\partial^2 p}{\partial\theta^2}+\frac{\omega_2}{3}\frac{1}{r}\frac{1}{\rho}\frac{\partial p}{\partial r}$$
$$+\frac{2\omega_2}{3}\frac{1}{\rho^2}\frac{\partial p}{\partial r}\frac{\partial\rho}{\partial r}-\frac{\omega_2}{3}\frac{1}{\rho^2}\frac{\partial p}{\partial z}\frac{\partial\rho}{\partial z}-\frac{\omega_2}{3}\frac{1}{r^2}\frac{1}{\rho^2}\frac{\partial p}{\partial\theta}\frac{\partial\rho}{\partial\theta}\Bigg], \tag{2.24}$$

$$\sigma^B_{\theta\theta}=\frac{\mu^2}{p}\Bigg[-\left(\frac{\omega_1}{3}-\frac{7\omega_2}{9}+\frac{1\omega_6}{9}\right)\left(\frac{\partial u}{\partial r}\right)^2+\left(\frac{\omega_1}{3}+\frac{2\omega_2}{9}-\frac{2\omega_6}{9}\right)\left(u\frac{\partial u}{\partial r}\right)$$
$$+\left(\frac{2\omega_1}{3}-\frac{14\omega_2}{9}+\frac{2\omega_6}{9}\right)\left(\frac{u}{r}\right)^2-\left(\frac{2\omega_2}{3}-\frac{\omega_6}{12}\right)\left(\frac{1}{r^2}\right)\left(\frac{\partial u}{\partial\theta}\right)^2$$
$$+\left(\frac{4\omega_2}{3}-\frac{\omega_6}{6}\right)\left(\frac{v}{r^2}\frac{\partial u}{\partial\theta}\right)+\left(\frac{\omega_2}{3}-\frac{\omega_6}{6}\right)\left(\frac{\partial u}{\partial z}\right)^2+\left(\frac{\omega_2}{3}+\frac{\omega_6}{12}\right)\left(\frac{\partial v}{\partial r}\right)^2$$
$$+\left(\frac{2\omega_2}{3}-\frac{\omega_6}{6}\right)\left(\frac{v}{r}\frac{\partial v}{\partial r}\right)-\left(\frac{2\omega_2}{3}-\frac{\omega_6}{12}\right)\left(\frac{v}{r}\right)^2+\left(\frac{2\omega_1}{3}-\frac{14\omega_2}{9}+\frac{2\omega_6}{9}\right)\left(\frac{1}{r}\frac{\partial v}{\partial\theta}\right)^2$$
$$+\left(\frac{4\omega_1}{3}-\frac{28\omega_2}{9}+\frac{4\omega_6}{9}\right)\left(\frac{u}{r^2}\frac{\partial v}{\partial\theta}\right)+\left(\frac{\omega_2}{3}+\frac{\omega_6}{12}\right)\left(\frac{\partial v}{\partial z}\right)^2+\left(\frac{\omega_2}{3}-\frac{\omega_6}{12}\right)\left(\frac{\partial w}{\partial r}\right)^2$$
$$-\left(\frac{2\omega_2}{3}-\frac{\omega_6}{12}\right)\left(\frac{1}{r}\frac{\partial w}{\partial\theta}\right)^2-\left(\frac{2\omega_1}{3}+\frac{4\omega_2}{9}-\frac{4\omega_6}{9}\right)\left(\frac{\partial u}{\partial r}\frac{\partial w}{\partial z}\right)+\left(\frac{4\omega_2}{3}-\frac{\omega_6}{3}\right)\frac{\partial u}{\partial z}\frac{\partial w}{\partial r}$$
$$-\left(\frac{2\omega_2}{3}-\frac{\omega_6}{6}\right)\left(\frac{1}{r}\frac{\partial u}{\partial\theta}\frac{\partial v}{\partial r}\right)+\left(\frac{\omega_1}{3}+\frac{2\omega_2}{9}-\frac{4\omega_6}{9}\right)\left(\frac{1}{r}\frac{\partial v}{\partial\theta}\frac{\partial w}{\partial z}\right)$$
$$+\left(\frac{\omega_1}{3}+\frac{2\omega_2}{9}-\frac{2\omega_6}{9}\right)\left(\frac{1}{r}\frac{\partial u}{\partial r}\frac{\partial v}{\partial\theta}\right)-\left(\frac{2\omega_2}{3}+\frac{\omega_6}{6}\right)\left(\frac{1}{r}\frac{\partial w}{\partial\theta}\frac{\partial v}{\partial z}\right)-\frac{2\omega_3}{3}\frac{R}{r}\frac{\partial T}{\partial r}$$
$$-\frac{\omega_3 R}{3}\frac{\partial^2 T}{\partial r^2}-\frac{\omega_3 R}{3}\frac{\partial^2 T}{\partial z^2}+\frac{2\omega_3}{3}\frac{R}{r^2}\frac{\partial^2 T}{\partial\theta^2}-\frac{\omega_4}{3}\frac{R}{p}\frac{\partial T}{\partial r}\frac{\partial p}{\partial r}-\frac{\omega_4}{3}\frac{R}{p}\frac{\partial T}{\partial z}\frac{\partial p}{\partial z}$$
$$+\frac{2\omega_4}{3}\frac{1}{p}\frac{R}{r^2}\frac{\partial T}{\partial\theta}\frac{\partial p}{\partial\theta}-\frac{\omega_5}{3}\frac{R}{T}\left(\frac{\partial T}{\partial r}\right)^2-\frac{\omega_5}{3}\frac{R}{T}\left(\frac{\partial T}{\partial z}\right)^2+\frac{2\omega_5}{3}\frac{R}{T}\frac{1}{r^2}\left(\frac{\partial T}{\partial\theta}\right)^2$$
$$+\left(\frac{\omega_1}{3}+\frac{2\omega_2}{9}-\frac{2\omega_6}{9}\right)\left(\frac{\partial w}{\partial z}\frac{u}{r}\right)-\left(\frac{\omega_1}{3}-\frac{7\omega_2}{9}+\frac{\omega_6}{9}\right)\left(\frac{\partial w}{\partial z}\right)^2+\frac{\omega_2}{3}\frac{1}{\rho}\frac{\partial^2 p}{\partial r^2}$$
$$+\frac{\omega_2}{3}\frac{1}{\rho}\frac{\partial^2 p}{\partial z^2}-\frac{2\omega_2}{3}\frac{1}{\rho}\frac{1}{r^2}\frac{\partial^2 p}{\partial\theta^2}-\frac{2\omega_2}{3}\frac{1}{\rho}\frac{1}{r}\frac{\partial p}{\partial r}-\frac{\omega_2}{3}\frac{1}{\rho^2}\frac{\partial p}{\partial r}\frac{\partial\rho}{\partial r}-\frac{\omega_2}{3}\frac{1}{\rho^2}\frac{\partial p}{\partial z}\frac{\partial\rho}{\partial z}$$
$$+\frac{2\omega_2}{3}\frac{1}{r^2}\frac{1}{\rho^2}\frac{\partial p}{\partial\theta}\frac{\partial\rho}{\partial\theta}\Bigg], \tag{2.25}$$

$$\sigma^B_{zz}=\frac{\mu^2}{p}\Bigg[-\left(\frac{\omega_1}{3}-\frac{7\omega_2}{9}+\frac{1\omega_6}{9}\right)\left(\frac{\partial u}{\partial r}\right)^2-\left(\frac{2\omega_1}{3}+\frac{4\omega_2}{9}-\frac{4\omega_6}{9}\right)\left(u\frac{\partial u}{\partial r}\right)$$
$$-\left(\frac{\omega_1}{3}-\frac{7\omega_2}{9}+\frac{\omega_6}{9}\right)\left(\frac{u}{r}\right)^2+\left(\frac{\omega_2}{3}-\frac{\omega_6}{6}\right)\left(\frac{1}{r^2}\right)\left(\frac{\partial u}{\partial\theta}\right)^2-\left(\frac{2\omega_2}{3}-\frac{\omega_6}{3}\right)\left(\frac{v}{r^2}\frac{\partial u}{\partial\theta}\right)$$
$$-\left(\frac{2\omega_2}{3}-\frac{\omega_6}{12}\right)\left(\frac{\partial u}{\partial z}\right)^2+\left(\frac{2\omega_2}{3}-\frac{\omega_6}{6}\right)\left(\frac{\partial v}{\partial r}\right)^2+\left(\frac{2\omega_2}{3}-\frac{\omega_6}{6}\right)\left(\frac{v}{r}\right)^2$$
$$-\left(\frac{\omega_1}{3}-\frac{7\omega_2}{9}+\frac{\omega_6}{9}\right)\left(\frac{1}{r}\frac{\partial v}{\partial\theta}\right)^2-\left(\frac{2\omega_1}{3}-\frac{14\omega_2}{9}+\frac{2\omega_6}{9}\right)\left(\frac{u}{r^2}\frac{\partial v}{\partial\theta}\right)$$
$$-\left(\frac{2\omega_2}{3}-\frac{\omega_6}{12}\right)\left(\frac{\partial v}{\partial z}\right)^2+\left(\frac{2\omega_2}{3}+\frac{\omega_6}{12}\right)\left(\frac{\partial w}{\partial r}\right)^2+\left(\frac{\omega_2}{3}-\frac{\omega_6}{12}\right)\left(\frac{1}{r}\frac{\partial w}{\partial\theta}\right)^2$$

$$
\begin{aligned}
&+\left(\frac{2\omega_1}{3}-\frac{14\omega_2}{9}+\frac{2\omega_6}{9}\right)\left(\frac{\partial w}{\partial z}\right)^2+\left(\frac{4\omega_2}{3}-\frac{\omega_6}{3}\right)\left(\frac{1}{r}\frac{\partial u}{\partial\theta}\frac{\partial v}{\partial r}\right)\\
&+\left(\frac{\omega_1}{3}+\frac{2\omega_2}{9}-\frac{2\omega_6}{9}\right)\frac{\partial w}{\partial z}\frac{\partial u}{\partial r}+\left(\frac{\omega_1}{3}+\frac{2\omega_2}{9}-\frac{2\omega_6}{9}\right)\left(\frac{1}{r}\frac{\partial v}{\partial\theta}\frac{\partial w}{\partial z}\right)\\
&+\left(\frac{-2\omega_2}{3}+\frac{\omega_6}{6}\right)\frac{\partial u}{\partial z}\frac{\partial w}{\partial r}-\left(\frac{2\omega_1}{3}+\frac{4\omega_2}{9}-\frac{4\omega_6}{9}\right)\left(\frac{1}{r}\frac{\partial u}{\partial r}\frac{\partial v}{\partial\theta}\right)+\left(4\frac{\omega_2}{3}+\frac{\omega_6}{3}\right)\frac{v}{r}\frac{\partial v}{\partial r}\\
&+\left(\frac{2\omega_2}{3}+\frac{\omega_6}{6}\right)\left(\frac{1}{r}\frac{\partial w}{\partial\theta}\frac{\partial v}{\partial z}\right)+\frac{\omega_4}{3}\frac{1}{p}\frac{R}{r^2}\frac{\partial T}{\partial\theta}\frac{\partial p}{\partial\theta}-\frac{\omega_5}{3}\frac{R}{T}\left(\frac{\partial T}{\partial r}\right)^2+\frac{2\omega_5}{3}\frac{R}{T}\left(\frac{\partial T}{\partial z}\right)^2\\
&-\frac{\omega_5}{3}\frac{R}{T}\frac{1}{r^2}\left(\frac{\partial T}{\partial\theta}\right)^2+\left(\frac{\omega_1}{3}+\frac{2\omega_2}{9}-\frac{2\omega_6}{9}\right)\left(\frac{\partial w}{\partial z}\frac{u}{r}\right)+\frac{\omega_2}{3}\frac{1}{\rho}\frac{\partial^2 p}{\partial r^2}-\frac{2\omega_2}{3}\frac{1}{\rho}\frac{\partial^2 p}{\partial z^2}\\
&+\frac{\omega_2}{3}\frac{1}{r^2}\frac{1}{\rho}\frac{\partial^2 p}{\partial\theta^2}+\frac{\omega_2}{3}\frac{1}{r}\frac{1}{\rho}\frac{\partial p}{\partial r}-\frac{\omega_2}{3}\frac{1}{\rho^2}\frac{\partial p}{\partial r}\frac{\partial\rho}{\partial r}+\frac{2\omega_2}{3}\frac{1}{\rho^2}\frac{\partial p}{\partial z}\frac{\partial\rho}{\partial z}\\
&-\frac{\omega_2}{3}\frac{1}{r^2}\frac{1}{\rho^2}\frac{\partial p}{\partial\theta}\frac{\partial\rho}{\partial\theta}-\frac{\omega_3}{3}\frac{R}{r}\frac{\partial T}{\partial r}-\frac{\omega_3}{3}R\frac{\partial^2 T}{\partial r^2}+\frac{2\omega_3 R}{3}\frac{\partial^2 T}{\partial z^2}-\frac{\omega_3}{3}\frac{R}{r^2}\frac{\partial^2 T}{\partial\theta^2}\\
&-\frac{\omega_4}{3}\frac{R}{p}\frac{\partial T}{\partial r}\frac{\partial p}{\partial r}+\frac{2\omega_4}{3}\frac{R}{p}\frac{\partial T}{\partial z}\frac{\partial p}{\partial z}\Bigg],
\end{aligned}
\tag{2.26}
$$

$$
\begin{aligned}
\sigma^B_{r\theta}=\sigma^B_{\theta r}=\ &\frac{\mu^2}{p}\Bigg[-\left(\frac{\omega_1}{2}-\frac{5\omega_2}{3}+\frac{\omega_6}{6}\right)\left(\frac{v}{r}\frac{\partial u}{\partial r}\right)+\left(\frac{\omega_1}{2}-\frac{2\omega_2}{3}+\frac{\omega_6}{6}\right)\left(\frac{u}{r^2}\frac{\partial u}{\partial\theta}\right)\\
&-\left(\frac{\omega_1}{2}-\frac{2\omega_2}{3}-\frac{\omega_6}{6}\right)\left(\frac{uv}{r^2}\right)+\left(\frac{\omega_1}{2}-\frac{5\omega_2}{3}+\frac{\omega_6}{6}\right)\left(\frac{u}{r}\frac{\partial v}{\partial r}\right)\\
&-\left(\frac{\omega_1}{2}-\frac{2\omega_2}{3}+\frac{\omega_6}{6}\right)\left(\frac{v}{r^2}\frac{\partial v}{\partial\theta}\right)-\left(\frac{\omega_1}{2}+\frac{\omega_2}{3}-\frac{\omega_6}{3}\right)\left(\frac{v}{r}\frac{\partial w}{\partial z}\right)\\
&+\left(\frac{\omega_1}{2}+\frac{\omega_2}{3}-\frac{\omega_6}{3}\right)\left(\frac{1}{r}\frac{\partial u}{\partial\theta}\frac{\partial w}{\partial z}\right)+\left(\frac{\omega_1}{2}-\frac{5\omega_2}{3}+\frac{\omega_6}{6}\right)\left(\frac{1}{r}\frac{\partial u}{\partial r}\frac{\partial u}{\partial\theta}\right)\\
&+\left(\frac{\omega_1}{2}+\frac{\omega_2}{3}-\frac{\omega_6}{3}\right)\left(\frac{\partial v}{\partial r}\frac{\partial w}{\partial z}\right)+\left(\frac{\omega_1}{2}-\frac{2\omega_2}{3}+\frac{\omega_6}{6}\right)\left(\frac{\partial u}{\partial r}\frac{\partial v}{\partial r}\right)\\
&+\left(\frac{\omega_1}{2}-\frac{2\omega_2}{3}+\frac{\omega_6}{6}\right)\left(\frac{1}{r^2}\frac{\partial u}{\partial\theta}\frac{\partial v}{\partial\theta}\right)+\left(\frac{\omega_1}{2}-\frac{5\omega_2}{3}+\frac{\omega_6}{6}\right)\left(\frac{1}{r}\frac{\partial v}{\partial r}\frac{\partial v}{\partial\theta}\right)\\
&-\left(\omega_2-\frac{\omega_6}{4}\right)\left(\frac{\partial v}{\partial z}\frac{\partial w}{\partial r}\right)-\left(\omega_2-\frac{\omega_6}{4}\right)\left(\frac{1}{r}\frac{\partial u}{\partial z}\frac{\partial w}{\partial\theta}\right)\\
&-\left(\omega_2-\frac{\omega_6}{4}\right)\left(\frac{1}{r}\frac{\partial w}{\partial r}\frac{\partial w}{\partial\theta}\right)+\omega_3\frac{R}{r}\frac{\partial^2 T}{\partial r\partial\theta}-\omega_3\frac{R}{r^2}\frac{\partial T}{\partial\theta}+\frac{\omega_4}{2}\frac{R}{r}\frac{1}{p}\frac{\partial p}{\partial\theta}\frac{\partial T}{\partial r}\\
&+\frac{\omega_4}{2}\frac{1}{r}\frac{R}{p}\frac{\partial p}{\partial r}\frac{\partial T}{\partial\theta}+\omega_5\frac{1}{T}\frac{R}{r}\frac{\partial T}{\partial r}\frac{\partial T}{\partial\theta}+\frac{\omega_6}{4}\frac{\partial u}{\partial z}\frac{\partial v}{\partial z}+\omega_2\frac{1}{r^2}\frac{1}{\rho}\frac{\partial p}{\partial\theta}-\omega_2\frac{1}{r}\frac{1}{\rho}\frac{\partial^2 p}{\partial r\partial\theta}\\
&+\frac{\omega_2}{2}\frac{1}{r}\frac{1}{\rho^2}\frac{\partial p}{\partial\theta}\frac{\partial\rho}{\partial r}+\frac{\omega_2}{2}\frac{1}{r}\frac{1}{\rho^2}\frac{\partial p}{\partial r}\frac{\partial\rho}{\partial\theta}\Bigg],
\end{aligned}
\tag{2.27}
$$

$$
\begin{aligned}
\sigma^B_{\theta z}=\sigma^B_{z\theta}=\ &\frac{\mu^2}{p}\Bigg[\left(\omega_2-\frac{\omega_6}{4}\right)\left(\frac{v}{r}\frac{\partial u}{\partial z}\right)+\left(\frac{\omega_1}{2}-\frac{5\omega_2}{3}+\frac{\omega_6}{6}\right)\left(\frac{u}{r}\frac{\partial v}{\partial z}\right)\\
&+\left(\omega_2-\frac{\omega_6}{4}\right)\left(\frac{v}{r}\frac{\partial w}{\partial r}\right)+\left(\frac{\omega_1}{2}-\frac{2\omega_2}{3}+\frac{\omega_6}{6}\right)\left(\frac{u}{r^2}\frac{\partial w}{\partial\theta}\right)
\end{aligned}
$$

$$+\left(\frac{\omega_1}{2}-\frac{2\omega_2}{3}+\frac{\omega_6}{6}\right)\left(\frac{\partial v}{\partial z}\frac{\partial w}{\partial z}\right)+\left(\frac{\omega_1}{2}+\frac{\omega_2}{3}-\frac{\omega_6}{3}\right)\left(\frac{\partial u}{\partial r}\frac{\partial v}{\partial z}\right)$$
$$-\left(\omega_2-\frac{\omega_6}{4}\right)\left(\frac{1}{r}\frac{\partial u}{\partial \theta}\frac{\partial u}{\partial z}\right)-\left(\omega_2-\frac{\omega_6}{4}\right)\left(\frac{\partial u}{\partial z}\frac{\partial v}{\partial r}\right)$$
$$+\left(\frac{\omega_1}{2}-\frac{5\omega_2}{3}+\frac{\omega_6}{6}\right)\left(\frac{1}{r}\frac{\partial v}{\partial z}\frac{\partial v}{\partial \theta}\right)-\left(\omega_2-\frac{\omega_6}{4}\right)\left(\frac{1}{r}\frac{\partial u}{\partial \theta}\frac{\partial w}{\partial r}\right)$$
$$+\frac{\omega_6}{4}\frac{\partial v}{\partial r}\frac{\partial w}{\partial r}+\left(\frac{\omega_1}{2}-\frac{5\omega_2}{3}+\frac{\omega_6}{6}\right)\left(\frac{1}{r}\frac{\partial w}{\partial z}\frac{\partial w}{\partial \theta}\right)$$
$$+\left(\frac{\omega_1}{2}+\frac{\omega_2}{3}-\frac{\omega_6}{3}\right)\left(\frac{1}{r}\frac{\partial u}{\partial r}\frac{\partial w}{\partial \theta}\right)+\left(\frac{\omega_1}{2}-\frac{2\omega_2}{3}+\frac{\omega_6}{6}\right)\left(\frac{1}{r^2}\frac{\partial v}{\partial \theta}\frac{\partial w}{\partial \theta}\right)$$
$$+\omega_3\frac{R}{r}\frac{\partial^2 T}{\partial\theta\partial z}+\frac{\omega_4}{2}\frac{1}{r}\frac{R}{p}\frac{\partial T}{\partial z}\frac{\partial p}{\partial \theta}+\frac{\omega_4}{2}\frac{1}{r}\frac{R}{p}\frac{\partial T}{\partial \theta}\frac{\partial p}{\partial z}+\omega_5\frac{1}{T}\frac{R}{r}\frac{\partial T}{\partial z}\frac{\partial T}{\partial \theta}$$
$$-\omega_2\frac{1}{r}\frac{1}{\rho}\frac{\partial^2 p}{\partial\theta\partial z}+\frac{\omega_2}{2}\frac{1}{r}\frac{1}{\rho^2}\frac{\partial p}{\partial \theta}\frac{\partial \rho}{\partial z}+\frac{\omega_2}{2}\frac{1}{r}\frac{1}{\rho^2}\frac{\partial p}{\partial z}\frac{\partial \rho}{\partial \theta}\Bigg], \tag{2.28}$$

$$\sigma_{rz}^B=\sigma_{zr}^B=\frac{\mu^2}{p}\Bigg[\left(\frac{\omega_1}{2}+\frac{\omega_2}{3}-\frac{\omega_6}{3}\right)\left(\frac{u}{r}\frac{\partial u}{\partial z}\right)+\left(\omega_2-\frac{\omega_6}{4}\right)\left(\frac{v}{r}\frac{\partial v}{\partial z}\right)$$
$$+\left(\frac{\omega_1}{2}+\frac{\omega_2}{3}-\frac{\omega_6}{3}\right)\left(\frac{u}{r}\frac{\partial w}{\partial r}\right)+\left(\frac{\omega_1}{2}-\frac{2\omega_2}{3}+\frac{\omega_6}{6}\right)\left(\frac{\partial u}{\partial z}\frac{\partial w}{\partial z}\right)$$
$$+\left(\frac{\omega_1}{2}-\frac{5\omega_2}{3}+\frac{\omega_6}{6}\right)\left(\frac{\partial u}{\partial r}\frac{\partial u}{\partial z}\right)-\left(\omega_2-\frac{\omega_6}{4}\right)\left(\frac{1}{r}\frac{\partial u}{\partial \theta}\frac{\partial v}{\partial z}\right)$$
$$-\left(\omega_2-\frac{\omega_6}{4}\right)\left(\frac{\partial v}{\partial z}\frac{\partial v}{\partial r}\right)+\left(\frac{\omega_1}{2}+\frac{\omega_2}{3}-\frac{\omega_6}{3}\right)\left(\frac{1}{r}\frac{\partial u}{\partial z}\frac{\partial v}{\partial \theta}\right)$$
$$+\left(\frac{\omega_1}{2}-\frac{5\omega_2}{3}+\frac{\omega_6}{6}\right)\left(\frac{\partial w}{\partial z}\frac{\partial w}{\partial r}\right)+\left(\frac{\omega_1}{2}-\frac{2\omega_2}{3}+\frac{\omega_6}{6}\right)\left(\frac{\partial u}{\partial r}\frac{\partial w}{\partial r}\right)$$
$$+\left(\frac{\omega_1}{2}+\frac{\omega_2}{3}-\frac{\omega_6}{3}\right)\left(\frac{1}{r}\frac{\partial v}{\partial \theta}\frac{\partial w}{\partial r}\right)-\frac{\omega_6}{4}\frac{v}{r^2}\frac{\partial w}{\partial \theta}+\frac{\omega_6}{4}\frac{1}{r^2}\frac{\partial u}{\partial \theta}\frac{\partial w}{\partial \theta}$$
$$-\left(\omega_2-\frac{\omega_6}{4}\right)\left(\frac{1}{r}\frac{\partial v}{\partial r}\frac{\partial w}{\partial \theta}\right)+\omega_3 R\frac{\partial^2 T}{\partial r\partial z}+\frac{\omega_4}{2}\frac{R}{p}\frac{\partial T}{\partial r}\frac{\partial p}{\partial z}+\frac{\omega_4}{2}\frac{R}{p}\frac{\partial p}{\partial r}\frac{\partial T}{\partial z}$$
$$+\omega_5\frac{R}{T}\frac{\partial T}{\partial r}\frac{\partial T}{\partial z}-\omega_2\frac{1}{\rho}\frac{\partial^2 p}{\partial r\partial z}+\frac{\omega_2}{2}\frac{1}{\rho^2}\frac{\partial p}{\partial z}\frac{\partial \rho}{\partial r}+\frac{\omega_2}{2}\frac{1}{\rho^2}\frac{\partial p}{\partial r}\frac{\partial \rho}{\partial z}\Bigg], \tag{2.29}$$

$$q_r^B=\frac{\mu^2}{\rho}\Bigg[-\left(\frac{2\theta_2}{3}-\frac{2\theta_4}{3}\right)\left(\frac{\partial^2 u}{\partial r^2}\right)+\frac{\theta_4}{2}\frac{\partial^2 u}{\partial z^2}+\frac{\theta_4}{2}\frac{1}{r^2}\frac{\partial^2 u}{\partial\theta^2}-\left(\frac{2\theta_2}{3}-\frac{2\theta_4}{3}\right)\left(\frac{1}{r}\frac{\partial u}{\partial r}\right)$$
$$+\left(\frac{2\theta_2}{3}-\frac{2\theta_4}{3}\right)\left(\frac{u}{r^2}\right)-\left(\frac{2\theta_2}{3}-\frac{\theta_4}{6}\right)\left(\frac{1}{r}\frac{\partial^2 v}{\partial r\partial\theta}\right)+\left(\frac{2\theta_2}{3}-\frac{7\theta_4}{6}\right)\left(\frac{1}{r^2}\frac{\partial v}{\partial \theta}\right)$$
$$-\left(\frac{2\theta_2}{3}-\frac{\theta_4}{6}\right)\left(\frac{\partial^2 w}{\partial r\partial z}\right)+\left(\theta_1-\frac{2\theta_2}{3}-\theta_5\right)\left(\frac{u}{r}\frac{1}{T}\frac{\partial T}{\partial r}\right)-\frac{3\theta_5}{2}\frac{v}{r^2}\frac{1}{T}\frac{\partial T}{\partial \theta}$$
$$-\frac{\theta_3}{3}\frac{u}{r}\frac{1}{p}\frac{\partial p}{\partial r}-\frac{\theta_3}{2}\frac{v}{r^2}\frac{1}{p}\frac{\partial p}{\partial \theta}+\left(\theta_1-\frac{8\theta_2}{3}+2\theta_5\right)\left(\frac{1}{T}\frac{\partial u}{\partial r}\frac{\partial T}{\partial r}\right)+\frac{3\theta_5}{2}\frac{1}{r^2}\frac{1}{T}\frac{\partial u}{\partial \theta}\frac{\partial T}{\partial \theta}$$
$$+\frac{3\theta_5}{2}\frac{1}{T}\frac{\partial u}{\partial z}\frac{\partial T}{\partial z}+\frac{\theta_3}{2}\frac{1}{p}\frac{\partial u}{\partial z}\frac{\partial p}{\partial z}+\frac{\theta_3}{2}\frac{1}{r^2}\frac{1}{p}\frac{\partial u}{\partial \theta}\frac{\partial p}{\partial \theta}-\frac{\theta_3}{3}\frac{1}{p}\frac{\partial w}{\partial z}\frac{\partial p}{\partial r}$$

$$+\left(\theta_1-2\theta_2+\frac{3\theta_5}{2}\right)\left(\frac{1}{r}\frac{1}{T}\frac{\partial v}{\partial r}\frac{\partial T}{\partial\theta}\right)-\frac{\theta_3}{3}\frac{1}{r}\frac{1}{RT}\frac{\partial v}{\partial\theta}\frac{\partial p}{\partial r}+\left(\theta_1-\frac{2\theta_2}{3}-\theta_5\right)\frac{1}{r}\frac{1}{T}\frac{\partial T}{\partial r}\frac{\partial v}{\partial\theta}$$
$$-\left(2\theta_2-\frac{3\theta_5}{2}\right)\left(\frac{1}{T}\frac{\partial w}{\partial r}\frac{\partial T}{\partial z}\right)+\frac{\theta_3}{2}\frac{1}{p}\frac{\partial w}{\partial r}\frac{\partial p}{\partial z}+\frac{1}{pr}\frac{\partial p}{\partial\theta}\frac{\partial v}{\partial r}\frac{\theta_3}{2}$$
$$+\left(\theta_1-\frac{2\theta_2}{3}-\theta_5\right)\left(\frac{1}{T}\frac{\partial w}{\partial z}\frac{\partial T}{\partial r}\right)+\frac{1}{p}\frac{\partial p}{\partial r}\frac{\partial u}{\partial r}\frac{2\theta_3}{3}\Bigg], \tag{2.30}$$

$$q_\theta^B=\frac{\mu^2}{\rho}\Bigg[\left(\frac{2\theta_2}{3}+\frac{7\theta_4}{6}\right)\left(\frac{1}{r^2}\frac{\partial u}{\partial\theta}\right)+\frac{\theta_4}{2}\frac{\partial^2 v}{\partial z^2}+\frac{\theta_4}{2}\frac{1}{p}\frac{\partial^2 v}{\partial r^2}-\left(\frac{2\theta_2}{3}-\frac{2\theta_4}{3}\right)\left(\frac{1}{r^2}\frac{\partial^2 v}{\partial\theta^2}\right)$$
$$+\frac{\theta_4}{2}\frac{1}{r}\frac{1}{p}\frac{\partial v}{\partial r}+\frac{\theta_3}{2}\frac{1}{p}\frac{\partial v}{\partial r}\frac{\partial p}{\partial r}-\frac{\theta_4}{2}\frac{v}{r^2}+\left(\theta_1-\frac{8\theta_2}{3}+2\theta_5\right)\left(\frac{u}{r^2}\frac{1}{T}\frac{\partial T}{\partial\theta}\right)-\frac{\theta_3}{2}\frac{v}{r}\frac{1}{p}\frac{\partial p}{\partial r}$$
$$+\frac{2\theta_3}{3}\frac{u}{r^2}\frac{1}{p}\frac{\partial p}{\partial\theta}-\left(\frac{2\theta_2}{3}-\frac{\theta_4}{6}\right)\left(\frac{\partial^2 u}{\partial r\partial\theta}\right)+\left(\theta_1-\frac{2\theta_2}{3}-\theta_5\right)\left(\frac{1}{r}\frac{1}{T}\frac{\partial u}{\partial r}\frac{\partial T}{\partial\theta}\right)$$
$$-\frac{\theta_3}{3}\frac{1}{r}\frac{1}{p}\frac{\partial u}{\partial r}\frac{\partial p}{\partial\theta}+\frac{\theta_3}{2}\frac{1}{r}\frac{1}{p}\frac{\partial u}{\partial\theta}\frac{\partial p}{\partial r}+\frac{3\theta_5}{2}\frac{1}{T}\frac{\partial v}{\partial r}\frac{\partial T}{\partial r}+\frac{3\theta_5}{2}\frac{1}{T}\frac{\partial v}{\partial z}\frac{\partial T}{\partial z}+\frac{\theta_3}{2}\frac{1}{p}\frac{\partial v}{\partial z}\frac{\partial p}{\partial z}$$
$$+\frac{2\theta_3}{3}\frac{1}{r^2}\frac{1}{RT}\frac{\partial v}{\partial\theta}\frac{\partial p}{\partial\theta}+\left(\theta_1-\frac{8\theta_2}{3}+2\theta_5\right)\left(\frac{1}{r^2}\frac{1}{T}\frac{\partial v}{\partial\theta}\frac{\partial T}{\partial\theta}\right)$$
$$-\left(\frac{2\theta_2}{3}-\frac{\theta_4}{6}\right)\left(\frac{1}{r}\frac{\partial^2 w}{\partial z\partial\theta}\right)+\left(\theta_1-\frac{2\theta_2}{3}-\theta_5\right)\frac{1}{r}\frac{1}{T}\frac{\partial w}{\partial z}\frac{\partial T}{\partial\theta}$$
$$-\left(2\theta_2-\frac{3\theta_5}{2}\right)\left(\frac{1}{r}\frac{1}{T}\frac{\partial w}{\partial\theta}\frac{\partial T}{\partial z}\right)-\frac{\theta_3}{3}\frac{1}{p}\frac{1}{r}\frac{\partial w}{\partial z}\frac{\partial p}{\partial\theta}+\frac{v}{r}\frac{1}{T}\frac{\partial T}{\partial r}\left(\frac{-3\theta_5}{2}+2\theta_2\right)$$
$$+\left(-2\theta_2+\frac{3\theta_5}{2}\right)\frac{1}{r}\frac{1}{T}\frac{\partial T}{\partial r}\frac{\partial u}{\partial\theta}\Bigg], \tag{2.31}$$

and

$$q_z^B=\frac{\mu^2}{\rho}\Bigg[-\left(\frac{2\theta_2}{3}-\frac{\theta_4}{6}\right)\left(\frac{1}{r}\frac{\partial u}{\partial z}\right)+\frac{\theta_4}{2}\frac{\partial^2 w}{\partial r^2}-\left(\frac{2\theta_2}{3}-\frac{2\theta_4}{3}\right)\left(\frac{\partial^2 w}{\partial z^2}\right)+\frac{\theta_4}{2}\frac{1}{r^2}\frac{\partial^2 w}{\partial\theta^2}$$
$$+\left(\theta_1-\frac{2\theta_2}{3}-\theta_5\right)\left(\frac{u}{r}\frac{1}{T}\frac{\partial T}{\partial z}\right)-\frac{\theta_3}{3}\frac{u}{r}\frac{1}{p}\frac{\partial p}{\partial z}+\left(\theta_1-\frac{2\theta_2}{3}-\theta_5\right)\left(\frac{1}{T}\frac{\partial u}{\partial r}\frac{\partial T}{\partial z}\right)$$
$$+\left(-2\theta_2+\frac{3\theta_5}{2}\right)\frac{1}{r}\frac{1}{T}\frac{\partial u}{\partial z}\frac{\partial T}{\partial r}-\frac{\theta_3}{3}\frac{1}{p}\frac{\partial u}{\partial r}\frac{\partial p}{\partial z}-\left(\frac{2\theta_2}{3}-\frac{\theta_4}{6}\right)\left(\frac{\partial^2 u}{\partial r\partial z}\right)+\frac{\theta_3}{2}\frac{1}{p}\frac{\partial u}{\partial z}\frac{\partial p}{\partial r}$$
$$-\left(\frac{2\theta_2}{3}-\frac{\theta_4}{6}\right)\left(\frac{1}{r}\frac{\partial^2 v}{\partial z\partial\theta}\right)+\frac{\theta_3}{2}\frac{1}{r}\frac{1}{p}\frac{\partial v}{\partial z}\frac{\partial p}{\partial\theta}+\left(\theta_1-\frac{2\theta_2}{3}-\theta_5\right)\left(\frac{1}{r}\frac{1}{T}\frac{\partial v}{\partial\theta}\frac{\partial T}{\partial z}\right)$$
$$-\frac{\theta_3}{3}\frac{1}{p}\frac{1}{r}\frac{\partial v}{\partial\theta}\frac{\partial p}{\partial z}+\frac{3\theta_5}{2}\frac{1}{T}\frac{\partial w}{\partial r}\frac{\partial T}{\partial r}+\frac{\theta_3}{2}\frac{1}{p}\frac{\partial w}{\partial r}\frac{\partial p}{\partial r}+\left(\theta_1-\frac{8\theta_2}{3}+2\theta_5\right)\left(\frac{1}{T}\frac{\partial w}{\partial z}\frac{\partial T}{\partial z}\right)$$
$$+\frac{2\theta_3}{3}\frac{1}{p}\frac{\partial w}{\partial z}\frac{\partial p}{\partial z}+\frac{\theta_3}{2}\frac{1}{r^2}\frac{1}{p}\frac{\partial w}{\partial\theta}\frac{\partial p}{\partial\theta}+\frac{3\theta_5}{2}\frac{1}{r^2}\frac{1}{T}\frac{\partial w}{\partial\theta}\frac{\partial T}{\partial\theta}$$
$$+\frac{\theta_4}{2}\frac{1}{r}\frac{\partial w}{\partial r}+\frac{1}{r}\frac{1}{T}\frac{\partial v}{\partial z}\frac{\partial v}{\partial\theta}\left(\frac{3\theta_5}{2}-2\theta_2\right)\Bigg]. \tag{2.32}$$

Notice that the above equations are in terms of six ω and five θ. The values of ω_i and θ_i for both Maxwellian and HS molecules are tabulated in table 1 (Zhong & Furumoto 1995). The transport coefficients depend upon the interaction model between

Coefficients	Maxwell molecules	Hard-sphere molecules
ω_1	$(4/3)[7/2-(T/\mu)\,\mathrm{d}\mu/\mathrm{d}t]$	$1.014\times(4/3)[7/2-(T/\mu)\,\mathrm{d}\mu/\mathrm{d}t]$
ω_2	2	2.028
ω_3	3	2.418
ω_4	0	0.681
ω_5	$3(T/\mu)\,\mathrm{d}\mu/\mathrm{d}t$	$0.806(T/\mu)\,\mathrm{d}\mu/\mathrm{d}t-0.990$
ω_6	8	7.424
θ_1	$(15/4)[7/2-(T/\mu)\,\mathrm{d}\mu/\mathrm{d}t]$	11.644
θ_2	$-45/8$	-5.822
θ_3	-3	-3.090
θ_4	3	2.418
θ_5	$3[35/4+(T/\mu)\,\mathrm{d}\mu/\mathrm{d}t]$	$1.627\times3[35/4+(T/\mu)\,\mathrm{d}\mu/\mathrm{d}t]$

TABLE 1. Coefficients for the Burnett stress and heat flux terms.

the molecules of the gas. The interaction potential is given by

$$\Psi(r)=\frac{\Phi_0}{\nu-1}r^{\nu-1}, \tag{2.33}$$

where r is the interatomic distance, Φ_0 is constant and ν is a number varying between $(1,\infty)$.

The dependence of the transport coefficients upon temperature and the interaction model is (Chapman & Cowling 1970; Jin & Slemrod 2001)

$$\mu = \frac{5\left(\dfrac{k_B m}{\Pi}\right)^{1/2}\left(\dfrac{2k_B}{\Phi}\right)^{2/(\nu-1)}T^s}{8\Gamma\left(2-\dfrac{2}{\nu-1}\right)\Psi(\nu)}, \tag{2.34}$$

$$k = \tfrac{15}{4}k_B\mu, \tag{2.35}$$

where k_B is the Boltzmann constant, m is the mass of a gas molecule, Γ is the gamma function, $\Psi(\nu)$ is tabulated in Chapman & Cowling (1970) and s is given as follows:

$$s=\frac{1}{2}+\frac{2}{\nu-1}. \tag{2.36}$$

In the current paper, two interaction models, HS ($\nu\to\infty$) and Maxwellian ($\nu=5$), have been utilized to present the solution of an axisymmetric problem in the subsequent section. The transport coefficients for the two sets of models with subscripts *HS* and *Max* referring to HS and Maxwellian molecules, respectively, are as follows Chapman & Cowling (1970):

$$\mu_{HS} = \frac{5}{16}\frac{\sqrt{k_B m T}}{\Pi^{1/2}\sigma^2}, \tag{2.37}$$

$$k_{HS} = \frac{75}{64\sigma^2}\left(\frac{k_B^3 T}{\Pi m}\right)^{1/2}, \tag{2.38}$$

$$\mu_{Max} = \frac{1}{3\Pi}\frac{2m}{\Phi}\frac{k_B T}{0.436}, \tag{2.39}$$

$$k_{Max} = \tfrac{5}{2}\mu_{Max} c_v. \tag{2.40}$$

Note that the above equations have been derived from the following stress tensor and heat flux vector (Chapman & Cowling 1970; Chang & Uhlenbeck 1948) by employing suitable coordinate transformations:

$$\sigma_{ij}^B = \frac{\mu^2}{p}\left\{\omega_1\frac{\partial v_k}{\partial x_k}S_{ij} - \omega_2\left[\frac{\partial}{\partial x_{\langle i}}\left(\frac{1}{\rho}\frac{\partial p}{\partial x_{j\rangle}}\right) + \frac{\partial v_k}{\partial x_{\langle i}}\frac{\partial v_{j\rangle}}{\partial x_k} + 2\frac{\partial v_k}{\partial x_{\langle i}}S_{j\rangle k}\right] + \omega_3 R\frac{\partial^2 T}{\partial x_{\langle i}\partial x_{j\rangle}}\right.$$
$$\left. + \omega_4 R\frac{\partial T}{\partial x_{\langle i}}\frac{\partial \ln p}{\partial x_{j\rangle}} + \theta_5\frac{R}{T}\frac{\partial T}{\partial x_{\langle i}}\frac{\partial T}{\partial x_{j\rangle}} + \omega_6 S_{k\langle i}S_{j\rangle k}\right\}, \tag{2.41}$$

$$q_i^B = \frac{\mu^2}{p}\left[\theta_1\frac{\partial v_k}{\partial x_k}\frac{\partial \ln T}{x_i} - \theta_2\left(\frac{2}{3}\frac{\partial^2 v_k}{\partial x_k\partial x_i} + \frac{2}{3}\frac{\partial v_k}{\partial x_k}\frac{\partial \ln T}{\partial x_i} + 2\frac{\partial v_k}{\partial x_i}\frac{\partial \ln T}{\partial x_k}\right)\right.$$
$$\left. + \theta_3 S_{ik}\frac{\partial \ln p}{\partial x_k} + \theta_4\frac{\partial S_{ik}}{\partial x_k} + 3\theta_5 S_{ik}\frac{\partial \ln T}{\partial x_k}\right], \tag{2.42}$$

$$S_{ij} = \frac{\partial v_{\langle i}}{\partial x_{j\rangle}} = \frac{1}{2}\frac{\partial v_i}{\partial x_j} + \frac{1}{2}\frac{\partial v_j}{\partial x_i} - \frac{1}{3}\frac{\partial v_k}{\partial x_k}\delta_{ij}. \tag{2.43}$$

These equations were derived by Zhong & Furumoto (1995) as a sub-part of the augmented Burnett equations. Zhong & Furumoto (1995) assumed the gas to be ideal and utilized the ideal gas equation *a priori*. We have independently derived these equations. Further, here the ideal gas equation has not been used to replace the pressure gradient with the density gradient. The accuracy of the derived equations can be checked by comparing these equations with the second-order terms of the augmented Burnett equations in Zhong & Furumoto (1995). We would like to point out that one of the coefficients reported as β_4 in Zhong & Furumoto (1995) is erroneous. It should be $-\omega_2$ and not $-\omega_2/2$ as stated therein. This can be confirmed from the presented equations; see also Agarwal *et al.* (2001).

3. Axisymmetric flow in a long microtube

The governing equations for the low-speed axisymmetric isothermal flow situation can be derived from (2.1)–(2.32). Here, Poiseuille flow in a long cylindrical tube is considered with walls at radius $D/2$ from the centre. The compressible viscous flow is assumed to be steady with negligible entry and exit effects. In the following subsections, we provide a solution for this flow within Burnett hydrodynamics.

3.1. *Solution procedure, boundary conditions and solution*

Singh *et al.* (2014*a*) recently developed an iterative scheme to derive an analytical solution of the augmented Burnett equations. In our algorithm, we start with the solution of a lower-order equation (NS in our case). The various terms of the higher-order equations (Burnett in our case) are evaluated numerically by substituting the assumed solution into the various terms of the higher-order equations, for a given case (location in the microtube and flow conditions). The order of each term, normalized by the highest-order term in the equation, therefore becomes available. The significant terms (magnitude $\geqslant 1\,\%$, say) are identified and the lower-order equation

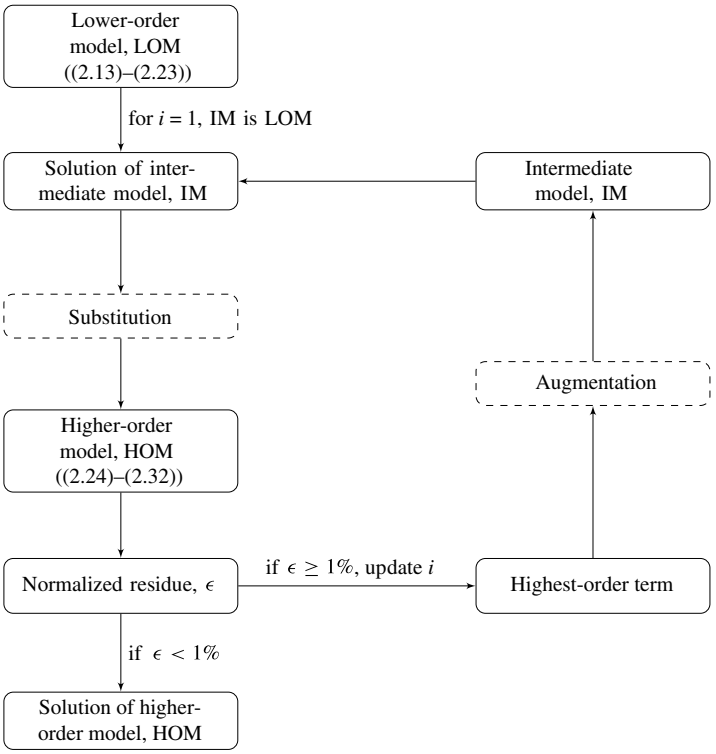

FIGURE 1. Iterative scheme to solve higher-order continuum equations. Note that IM will involve more terms than the NS equations but fewer terms than the Burnett equations.

is modified to include these new terms. This new lower-order (or intermediate) equation is again solved analytically and the entire exercise is repeated. The above exercise is repeated until all terms from the higher-order equations get added to the intermediate equations (and therefore the intermediate and higher-order equations become identical) or there are no remaining terms with a significant contribution. Note that the above exercise needs to be repeated for alternative locations in the microtube and flow conditions. Figure 1 shows the implementation procedure of the scheme, in which LOM corresponds to the NS equations, IM to the augmented (obtained after adding terms to the NS equations) set of equations, and HOM to higher-order continuum equations. In this work, we take the approach forwards and implement it for cylindrical Poiseuille flow. The solution of Sreekanth (1968) has been utilized as the starting solution (solution of LOM; figure 1) for the problem.

The second-order slip boundary condition has been used to derive the solution

$$w_{slip} = -C_1\lambda\left(\frac{\partial w}{\partial r}\right)_{wall} - C_2\lambda^2\left(\frac{\partial^2 w}{\partial r^2}\right)_{wall}, \tag{3.1}$$

where w_{slip} is the velocity slip, and C_1 and C_2 are slip coefficients (their values are taken from the literature, as discussed later).

Note that the Burnett equations are third-order equations and therefore require additional boundary conditions compared to the second-order NS equations. The requirement of having to prescribe additional boundary conditions can however be

deferred till a third-order derivative term enters the intermediate equation. In the present case, the solution converges after a single iteration, which shows that the solution of the NS equations is also a solution of the Burnett equations for Poiseuille flow.

The solutions for streamwise velocity (w), radial velocity (u) and pressure field (p) are as follows:

streamwise velocity

$$\frac{w}{\bar{w}} = \frac{4C_1Kn + 8C_2Kn^2 + 1 - 4\left(\frac{r}{D}\right)^2}{\frac{1}{2} + 4C_1Kn + 8C_2Kn^2}, \tag{3.2}$$

radial velocity

$$u = \frac{\mathrm{d}p}{\mathrm{d}z}\frac{Re\mu RT}{p^2}\left[\frac{4C_1Kn + 16C_2Kn^2}{(\frac{1}{2} + 4C_1Kn + 8C_2Kn^2)^2}\right]\left[-\frac{r}{4D} + \left(\frac{r}{D}\right)^3\right], \tag{3.3}$$

pressure

$$\begin{aligned}&\left(\frac{p}{p_0}\right) - 1 + 16C_1Kn_0\left(\frac{p}{p_0} - 1\right) + 32C_2Kn_0^2\log\frac{p}{p_0} \\ &\quad + 2Re^2\beta\chi\left\{8C_1Kn_0\left(\frac{p_0}{p} - 1\right) + 8C_2Kn_0^2\left[\left(\frac{p_0}{p}\right)^2 - 1\right] - \log\frac{p}{p_0}\right\} \\ &= -64Re\beta\frac{z - z_0}{D},\end{aligned} \tag{3.4}$$

where

$$\chi = \frac{\frac{1}{3} + 4C_1Kn + 16C_1^2Kn^2 + 8C_2Kn^2 + 64C_2^2Kn^4 + 64C_1C_2Kn^3}{(\frac{1}{2} + 4C_1Kn + 8C_2Kn^2)^2}, \tag{3.5}$$

$$\beta = \frac{\mu^2RT}{p_0^2D^2}. \tag{3.6}$$

In the above equations, Re is the Reynolds number, Kn_0 is the outlet Knudsen number, p_0 is the outlet pressure and z_0 is the reference location. Further, χ is an integral of the square of the streamwise velocity normalized with the mean velocity over the cross-section (its value lies between 1 and 1.2 over the full range of local Knudsen number Kn, when an average value of Knudsen number at the inlet and outlet is used). The area-averaged velocity ($\bar{w}$) at any cross-section has been used for normalizing the velocities.

The following free molecular relation for mass flow rate has been utilized for normalization:

$$\dot{m_{FM}} = \frac{4}{3}\left(\frac{D}{2}\right)^3\frac{p_i - p_o}{L}\sqrt{\frac{2\pi}{RT}}. \tag{3.7}$$

The non-dimensional mass flow rate can be obtained based on the solution in (3.2)–(3.4).

Notice that the streamwise velocity profile is parabolic. The coefficients of the parabola are a function of streamwise position due to density variation; this gives rise to a finite (but small) lateral velocity.

An assumption of isothermal flow condition has been made in the above derivation; this is not a particularly severe assumption. For example, as experimentally demonstrated by Varade, Agrawal & Pradeep (2014), the temperature rise in a tube with inlet to outlet pressure ratio of about eight at $Kn = 0.07$ is less than 1 °C; note that these measurements are with rarefied gas flow and the fully developed length is 53 times the tube diameter in their case. Our experience with measurements in a microchannel has also shown that the temperature rise is negligibly small in long microchannels (length to hydraulic diameter ratio of approximately 140). The solution in (3.2)–(3.6) is therefore valid over a wide range of practical cases.

3.2. *Results and discussion*

The intermediate model, IM (see figure 1) may not add up to the complete set of the Burnett equations on augmentation. Some terms may remain neglected, as a consequence of which the analytical solution may not satisfy the Burnett equations exactly. This can be visualized from the error plotted in figure 2. The error plotted is the residue obtained by substituting the solution into the governing equations normalized with the leading-order term. The analytical solutions in (3.2)–(3.6) satisfy the full set of Burnett equations and second-order slip boundary conditions (3.1) up to $Kn \leqslant 1.3$ within an error norm of $\pm 1\,\%$. The error is evaluated for the axial momentum equation. The error is plotted with respect to the local Knudsen number at three different radial locations $r = 0$, $D/4$ and approximately $D/2$. The analysis is presented at various locations to capture the effect of various terms whose magnitudes vary with location and flow conditions. Similar results were obtained for other cases not shown here. The plot shows the results of the error plotted with the Burnett equations under the assumption of Maxwellian as well as HS molecules. Note that the value of the transport coefficients in (2.37)–(2.40) vary depending on whether the molecule has been assumed to be Maxwellian or HS; this variation has been accounted for while plotting the solution in figure 2(*a*,*b*). The solution is exact for $Kn \leqslant 0.3$, beyond which the error starts increasing.

Figure 2(*a*) shows the error obtained with the slip coefficients proposed by Cercignani & Daneri (1963) under the assumption of molecules being HS and Maxwellian. The error is evaluated at the centre of the microtube. The Cercignani & Daneri (1963) coefficients with the HS model cover the maximum Knudsen range, $Kn = [0, 1.35]$. Similar errors were obtained at other locations with the coefficients given by Ewart *et al.* (2007) as shown in figure 2(*b*). Clearly, the error is within $\pm 1\,\%$ for Kn as high as 1.35 in figure 2(*b*). No drastic change in error is obtained with different slip coefficients (figure 2*c*). However, this finding should not be used to judge the correctness of the values of the slip coefficients.

The nature of the error curve (with Ewart's coefficients) is similar to that reported by Singh *et al.* (2014*a*) for flow in a microchannel with the augmented Burnett equations. The error changes its sign at $Kn = 0.3$ in the present case as apparent from figure 2(*d*). The term $(\mu^2/p)(\omega_2/3)(1/\rho)\,\partial^2 p/\partial z^2$ is responsible for the change in the sign of the error; a similar observation is reported by Singh *et al.* (2014*a*) for planar Poiseuille flow. It is proposed that an increase in the Knudsen number enhances the contribution of density gradients, which increases diffusion of volume (and momentum); see also Brenner (2005), Dongari, Sharma & Durst (2009), Dongari, Durst & Chakraborty (2010), Dadzie & Reese (2012) and Singh *et al.* (2014*a*).

The error curve obtained after substituting the solution in the NS equations has also been plotted. The error curve for the NS equations has opposite sign to that

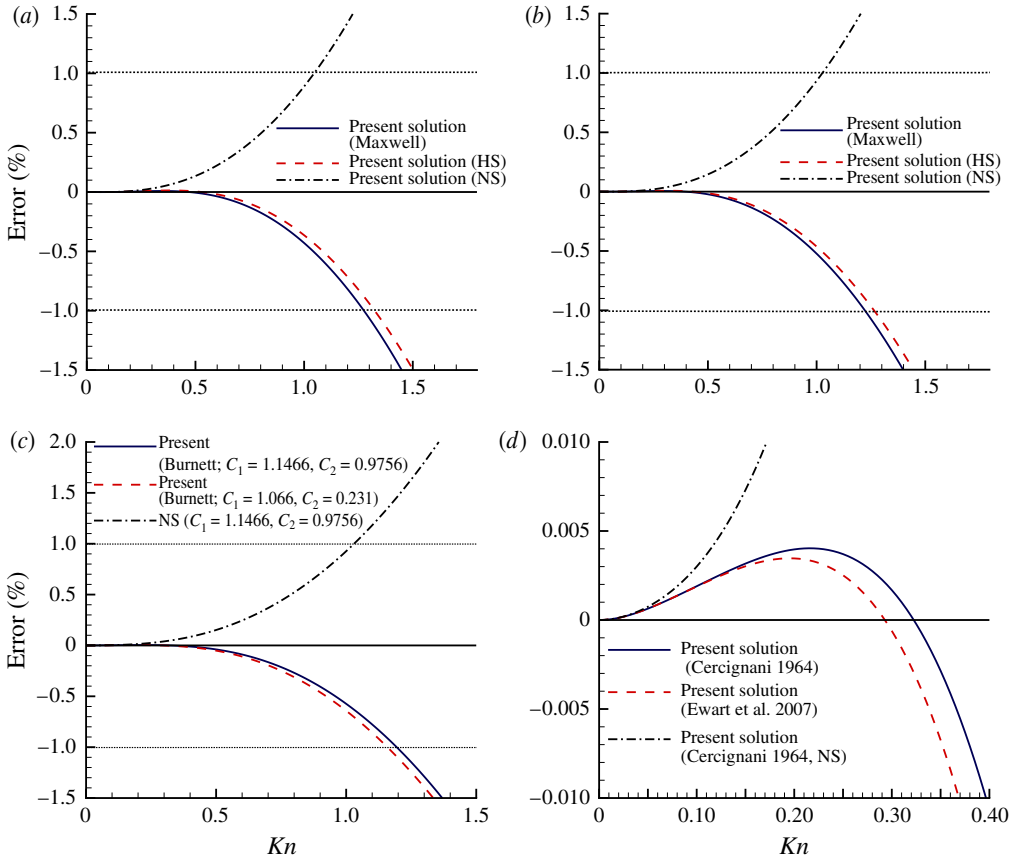

FIGURE 2. (Colour online) Error (in per cent) versus Knudsen number for the full Burnett equations and the NS equations at (*a*) $r = 0$, (*b*) $r = D/4$, (*c*) $r \approx D/2$ and (*d*) $r \approx D/2$. (*a*) Gas molecules assumed as HS or Maxwellian, with $C_1 = 1.1466$, $C_2 = 0.9756$. (*b*) Same as (*a*) but with $C_1 = 1.066$, $C_2 = 0.231$. (*c*) Gas molecules assumed as Maxwellian with two different sets of slip coefficients. (*d*) Same as (*c*) showing a zoomed view.

of the Burnett equations (figure 2*c*). Although the NS equations can be extended in to the slip regime with second-order slip boundary conditions, their applicability is restricted to $Kn \leqslant 1.0$, well below the transition regime. The divergence of the error in the transition regime makes the applicability of the NS equations questionable in the transition regime.

In order to further validate the solution, we compare the proposed analytical solution against experimental data. Figure 3 shows a comparison of the normalized mass flow rate derived from our model with different available models plotted against inlet Knudsen number (Kn_i). Knudsen (1909) averaged out the mass flow rate in the free molecular limit and for continuous incompressible flow in a pipe with the Hagen–Poiseuille relation to arrive at the mass flow rate for slip and transition regimes. The Tison (1993) model is the best-fitting approximation of the experimental results. Beskok & Karniadakis (1999) modified the Knudsen model and added a rarefaction coefficient as a function of Knudsen number to it. The results for the mass flow rate show that the solution is well applicable up to $Kn \leqslant 2$. This strengthens the claim

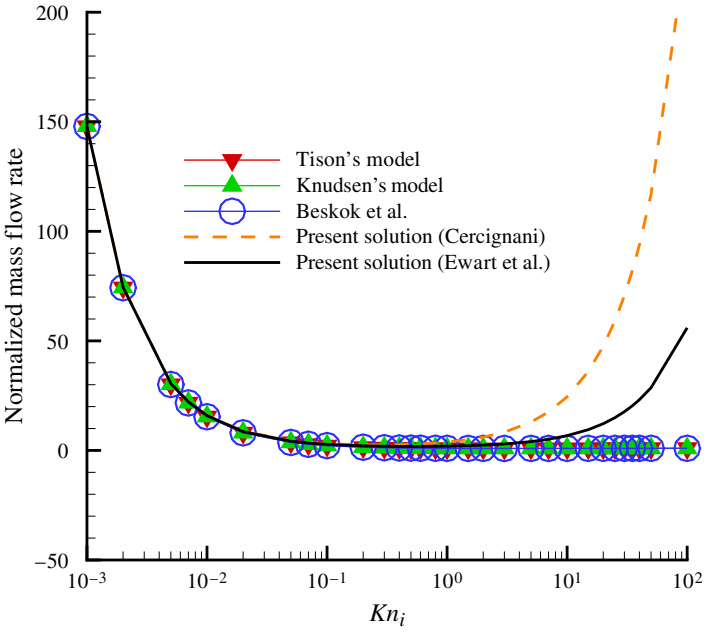

FIGURE 3. (Colour online) Normalized mass flow rate against inlet Knudsen number (Kn_i). Note that all the results plotted are with $p_d/p_i \sim 0$ and $L/D_h = 1363$.

that rarefied gas flows in the transition regime can be well captured by means of higher-order continuum models such as the Burnett equations. Further, the proposed solution captures the non-monotonic behaviour (the Knudsen minima) correctly. Although employing different sets of slip coefficients has a similar effect, the results for mass flow rate are slightly better with the Ewart *et al.* (2007) coefficients. As shown experimentally by Sreekanth (1968), the applicability of a solution to relatively higher Knudsen number can be obtained with more appropriate boundary conditions and slip coefficients. Ewart's slip coefficients have been utilized for all the subsequent analysis.

The contribution of the Burnett shear stress term to the overall shear stress can be seen from figure 4. The figure shows the relative magnitude of the Burnett shear stress compared to the NS shear stress, i.e. $\sigma_{rz}^{B}/\sigma_{rz}^{NS}$. The figure shows that the contribution of the Burnett shear stress term is negligible till $Kn \leqslant 0.5$. The primary contributing terms to the shear stress at the wall can be readily obtained from (2.29). Under the imposed boundary conditions and assumptions, the following terms are significant in σ_{rz}^{B}:

$$\left(\frac{\mu^2}{p}\right)\left(\frac{\omega_1}{2}-\frac{5\omega_2}{3}+\frac{\omega_6}{6}\right)\left(\frac{\partial w}{\partial z}\frac{\partial w}{\partial r}\right), \quad \left(\frac{\mu^2}{p}\right)\left(\frac{\omega_1}{2}-\frac{2\omega_2}{3}+\frac{\omega_6}{6}\right)\left(\frac{\partial u}{\partial r}\frac{\partial w}{\partial r}\right). \tag{3.8a,b}$$

The contributing terms in the present case involve the product of strain rates and cross-derivatives, which are part of the shear strain rate in the context of a fluid particle (Landau & Lifshitz 1958).

We now analyse the role of axially diffused volume, which can contribute to the overall momentum diffusion of the gas. This can provide an insight into the underlying reasons for the Knudsen paradox/minima (Knudsen 1909). To this end, we present the

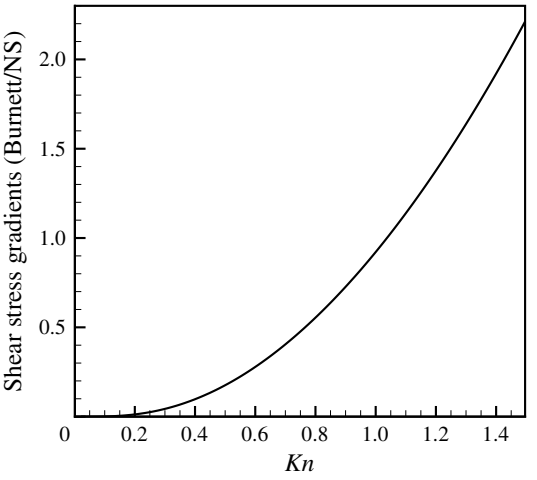

FIGURE 4. Burnett shear stress normalized with NS shear stress (in per cent) versus Knudsen number.

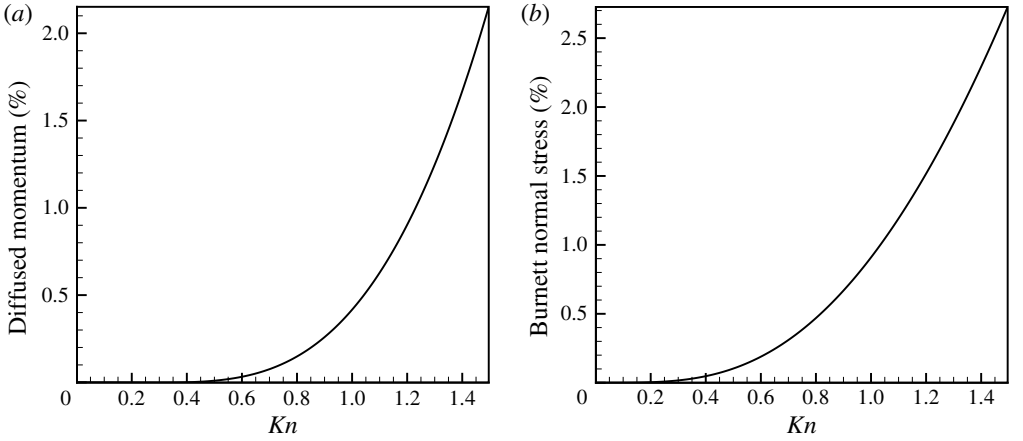

FIGURE 5. (*a*) Diffused momentum (in per cent) versus Knudsen number and (*b*) Burnett stress normalized with pressure gradient (in per cent) versus Knudsen number at wall. Note that quantities have been plotted by normalizing with pressure gradient.

diffusion terms of the Burnett stress terms. The gradients of the two terms contributing to the axial diffusion have been identified from (2.26). These terms involving density and pressure gradients are

$$\frac{\mu^2}{p}\frac{2\omega_2}{3}\frac{1}{\rho^2}\frac{\mathrm{d}p}{\mathrm{d}z}\frac{\mathrm{d}\rho}{\mathrm{d}z}, \qquad -\frac{\mu^2}{p}\frac{2\omega_2}{3}\frac{1}{\rho}\frac{\mathrm{d}^2p}{\mathrm{d}z^2}. \tag{3.9a,b}$$

The sum of the gradients of these terms along the axial coordinate, normalized with pressure gradient, lead to volume diffusion, thereby contributing to additional momentum diffusion. Figure 5(*a*) shows that the magnitude of this diffused momentum is insignificant at lower Knudsen numbers ($Kn < 0.5$); however, its contribution increases rapidly with increase in the Knudsen number. The phenomenon

of axial diffusion of volume and momentum is a consequence of strong density, pressure or temperature gradients at higher Knudsen number (Brenner 2005; Dadzie & Reese 2012; Dongari *et al.* 2009, 2010; Singh *et al.* 2014*a*). The phenomenon of volume diffusion leads to an effect that can be captured by terms of Burnett order. Figure 5(*b*) shows the contribution of the Burnett normal stresses normalized with pressure gradient. It incorporates all the Burnett normal stress terms in the stress tensor. This plot shows that all other terms in the Burnett normal stress other than the mentioned contributing terms have a marginal role.

3.3. *Reduced Burnett equations for Poiseuille flow in a microtube*

Based on a rigorous analysis of the order of magnitude of each term in the Burnett equations, we suggest the following reduced set of equations:

$$\frac{1}{r}\frac{\partial r\rho u}{\partial r}+\frac{\partial \rho w}{\partial z}=0, \tag{3.10}$$

$$\frac{1}{r}\frac{\partial r(\rho wu+\sigma_{rz})}{\partial r}+\frac{\partial(\rho ww+p+\sigma_{zz})}{\partial z}=0, \tag{3.11}$$

$$\frac{1}{r}\frac{\partial r(\rho uu+p+\sigma_{rr})}{\partial r}+\frac{\partial(\rho uw+\sigma_{zr})}{\partial z}=0, \tag{3.12}$$

$$\sigma_{rz}=-\mu\left(\frac{\partial w}{\partial r}\right)+\frac{\mu^2}{p}\left[\left(\frac{\omega_1}{2}-\frac{5\omega_2}{3}+\frac{\omega_6}{6}\right)\left(\frac{\partial w}{\partial z}\frac{\partial w}{\partial r}\right)+\left(\frac{\omega_1}{2}-\frac{2\omega_2}{3}+\frac{\omega_6}{6}\right)\left(\frac{\partial u}{\partial r}\frac{\partial w}{\partial r}\right)\right], \tag{3.13}$$

$$\sigma_{zz}=-\mu\left(\delta_1\frac{\partial w}{\partial z}\right)+\frac{\mu^2}{p}\left[\left(\frac{2\omega_1}{3}-\frac{14\omega_2}{9}+\frac{2\omega_6}{9}\right)\left(\frac{\partial w}{\partial z}\right)^2-\frac{2\omega_2}{3}\frac{1}{\rho}\frac{\partial^2 p}{\partial z^2}+\frac{2\omega_2}{3}\frac{1}{\rho^2}\frac{\partial p}{\partial z}\frac{\partial \rho}{\partial z}\right], \tag{3.14}$$

$$\sigma_{rr}=\frac{\mu^2}{p}\left[-\left(\frac{2\omega_1}{3}-\frac{14\omega_2}{9}+\frac{2\omega_6}{9}\right)\left(\frac{\partial u}{\partial r}\right)^2\right], \tag{3.15}$$

$$p=\rho RT. \tag{3.16}$$

The simplification comes because other terms do not contribute significantly for the considered problem. Equations (3.10)–(3.16) should work for the same set of assumptions for which the solution in (3.2)–(3.6) has been provided. However, the solutions provided above are not the direct solution of (3.10)–(3.16); it is reasonable to expect them to work for a larger Knudsen envelope and also higher Mach number if solved numerically. It is worthwhile to underscore that the above equations are applicable for $Kn\leqslant 0.5$. For $Kn>0.5$, some of the neglected terms become significant and therefore the addition of more terms becomes necessary. The exact Knudsen envelope over which the above equations are applicable will be known after actually solving them numerically. It appears that not all the Burnett terms will become significant till a Knudsen number as high as 5. Solving the reduced set of equations is easier because of fewer significant terms in the equations. It can be checked if the reduced set does not suffer from the stability issues associated with the Burnett equations.

4. Conclusions

Three-dimensional generalized conventional Burnett equations in cylindrical coordinates have been derived from Cartesian tensors with appropriate coordinate transformation. The stress and heat flux terms for both Maxwellian as well as HS molecules are reported. The various terms in the equations have been stated explicitly so that these can be utilized in the future with relative ease.

Further, we propose a solution of the Burnett equations for the axisymmetric isothermal flow situation in a long microtube. The challenge of an additional boundary condition to solve these equations has been met by employing an iterative solution methodology. The analytical solution is shown to satisfy the full set of Burnett equations exactly up to $Kn \leqslant 0.3$, beyond which it can be successfully employed for $Kn \leqslant 1.35$ with an error lying within $\pm 1\,\%$. The error is because the solution satisfies only the more significant terms in the equation. The solution, which is applicable for a reasonable part of the transition regime, clearly scores over the existing NS- and Burnett-based solutions.

We have compared the normalized mass flow rate with experimental results in the literature. A reasonable match has been obtained for $Kn \leqslant 2.2$, covering the entire continuum and slip regimes along with a substantial part of the transition regime. The same solution satisfies other forms of the Burnett equations (original and conventional) as well. Note that no variation in slip coefficients or the introduction of wall scaling functions into constitutive relations have been employed here to arrive at the solution.

A detailed quantitative analysis has been presented for the axial diffusion of momentum at higher Knudsen number. We have presented the significance of higher-order terms quantitatively in the scope of shear stress. These insights have helped us propose a reduced set of equations pertinent to flow in a microtube. Instead of the entire Burnett equation, these reduced equations can be solved numerically to obtain a solution for higher Knudsen numbers.

We claim that our solution is the first analytical solution of the Burnett equations for cylindrical Poiseuille flow. Since the solution satisfies the governing equation and the boundary conditions, the solution is deemed to be correct; its correctness is further demonstrated by comparison against experimental data for flow in the transition regime. We believe that this solution is significant, as not many analytical solutions are available for flow in the transition regime; these results can be utilized for benchmarking numerical simulations and other results in future. We expect that our observation of the Burnett equations providing correct analytical solution for Knudsen number greater than one (i.e. well within the transition regime) should lend some additional credence for employing these equations for modelling microscale flows.

REFERENCES

AGRAWAL, A. & DONGARI, N. 2012 Application of Navier–Stokes equations to high Knudsen number flow in a fine capillary. *Intl J. Microscale Nanoscale Therm. Fluid Transp. Phenomena* **3** (2), 125–130.

AGARWAL, R. K., YUN, K. Y. & BALAKRISHNAN, R. 2001 Beyond Navier–Stokes Burnett equations for flows in the continuum transition regime. *Phys. Fluids* **13**, 3061–3085; (Erratum: 2002 *Phys. Fluids* **14**, 1818).

BAO, F. & LIN, J. 2008 Burnett simulations of gas flow in microchannels. *Fluid Dyn. Res.* **40** (9), 679–694.

BESKOK, A. & KARNIADAKIS, G. E. 1999 Report: a model for flows in channels, pipes, and ducts at micro and nano scales. *Microscale Therm. Engng* **3** (1), 43–77.

BOBYLEV, A. V. 1982 The Chapman–Enskog and Grad methods for solving the Boltzmann equation. *Dokl. Akad. Nauk SSSR* **27**, 29–31.

BRENNER, H. 2005 Navier–Stokes revisited. *Physica* A **349** (1), 60–132.

CERCIGNANI, C. & DANERI, A. 1963 Flow of a rarefied gas between two parallel plates. *J. Appl. Phys.* **34** (12), 3509–3513.

CHANG, W. & UHLENBECK, G. E. 1948 On the transport phenomena in rarified gases. *Tech Rep.* DTIC Document.

CHAPMAN, S. & COWLING, T. G. 1970 *The Mathematical Theory of Non-Uniform Gases: An Account of the Kinetic Theory of Viscosity, Thermal Conduction and Diffusion in Gases*. Cambridge University Press.

COMEAUX, K. A., CHAPMAN, D. R. & MACCORMACK, R. W. 1995 An analysis of the Burnett equations based on the second law of thermodynamics. In *Proceedings of the 33rd AIAA, Aerospace Sciences Meeting and Exhibit, Reno, NV. AIAA paper* 95-0415.

DADZIE, S. K. 2013 A thermo-mechanically consistent Burnett regime continuum flow equation without Chapman–Enskog expansion. *J. Fluid Mech.* **716**, R6.

DADZIE, S. K. & REESE, J. M. 2012 Analysis of the thermomechanical inconsistency of some extended hydrodynamic models at high Knudsen number. *Phys. Rev.* E **85**, 041202.

DONGARI, N., DURST, F. & CHAKRABORTY, S. 2010 Predicting microscale gas flows and rarefaction effects through extended Navier–Stokes–Fourier equations from phoretic transport considerations. *Microfluid Nanofluid.* **9** (4–5), 831–846.

DONGARI, N., SHARMA, A. & DURST, F. 2009 Pressure-driven diffusive gas flows in micro-channels: from the Knudsen to the continuum regimes. *Microfluid. Nanofluid.* **6** (5), 679–692.

EWART, T., PERRIER, P., GRAUR, I. A. & MEOLANS, J. G. 2007 Mass flow rate measurements in a microchannel, from hydrodynamic to near free molecular regimes. *J. Fluid Mech.* **584**, 337–356.

GARCÍA-COLÍN, L. S., VELASCO, R. M. & URIBE, F. J. 2008 Beyond the Navier–Stokes equations: Burnett hydrodynamics. *Phys. Rep.* **465** (4), 149–189.

GATIGNOL, R. 2012 Asymptotic modelling of flows in microchannel by using Navier–Stokes or Burnett equations and comparison with DSMC simulations. *Vacuum* **86** (12), 2014–2028.

GRAD, H. 1949 On the kinetic theory of rarefied gases. *Commun. Pure Appl. Maths* **2**, 331–407.

GU, X.-J. & EMERSON, D. R. 2009 A high-order moment approach for capturing non-equilibrium phenomena in the transition regime. *J. Fluid Mech.* **636**, 177–216.

JIN, S. & SLEMROD, M. 2001 Regularization of the Burnett equations via relaxation. *J. Stat. Phys.* **103** (5–6), 1009–1033.

KARNIADAKIS, G., BESKOK, A. & ALURU, N. 2005 *Microflows and Nanoflows: Fundamentals and Simulation*. Springer.

KNUDSEN, M. 1909 Die Gesetze der Molekularströmung und der inneren Reibungsströmung der Gase durch Röhren. *Ann. Phys.* **333** (1), 75–130.

LANDAU, L. D. & LIFSHITZ, E. M. 1958 *Fluid Mechanics*. Pergamon.

PONG, K., HO, C. M., LIU, J. & TAI, Y. C. 1994 Non-linear pressure distribution in uniform microchannels. In *Proceedings of Application of Microfabrication to Fluid Mechanics, ASME Winter Annual Meeting, Chicago*, pp. 51–56.

SINGH, N., DONGARI, N. & AGRAWAL, A. 2014*a* Analytical solution of plane Poiseuille flow within burnett hydrodynamics. *Microfluid Nanofluid.* **16** (1–2), 403–412.

SINGH, N., GAVASANE, A. & AGRAWAL, A. 2014*b* Analytical solution of plane Couette flow in the transition regime and comparison with direct simulation Monte Carlo data. *Comput. Fluids* **97**, 177–187.

SREEKANTH, A. K. 1968 Slip flow through long circular tubes. In *Rarefied Gas Dynamics* (ed. L. Trilling & H. Y. Wachman). Academic Press.

STEVANOVIC, N. D. 2007 A new analytical solution of microchannel gas flow. *J. Micromech. Microengng* **17** (8), 1695–1702.

STRUCHTRUP, H. & TORRILHON, M. 2003 Regularization of Grad's 13 moment equations: derivation and linear analysis. *Phys. Fluids* **15**, 2668–2680.

TISON, S. A. 1993 Experimental data and theoretical modeling of gas flows through metal capillary leaks. *Vacuum* **44** (11), 1171–1175.

URIBE, F. J. & GARCIA, A. L. 1999 Burnett description for plane Poiseuille flow. *Phys. Rev.* E **60**, 4063–4078.

VARADE, V., AGRAWAL, A. & PRADEEP, A. M. 2014 Behaviour of rarefied gas flow near the junction of a suddenly expanding tube. *J. Fluid Mech.* **739**, 363–391.

XUE, H. & JI, H. 2003 Prediction of flow and heat transfer characteristics in micro-Couette flow. *Microscale Therm. Engng* **7** (1), 51–68.

YANG, Z. & GARIMELLA, S. V. 2009 Rarefied gas flow in microtubes at different inlet–outlet pressure ratios. *Phys. Fluids* **21**, 052005.

ZHONG, X. 1991 Development and computation of continuum higher order constitutive relations for high-altitude hypersonic flow. PhD thesis, Stanford University.

ZHONG, X. & FURUMOTO, G. H. 1995 Augmented Burnett-equation solutions over axisymmetric blunt bodies in hypersonic flow. *J. Spacecr. Rockets* **32** (4), 588–595.

ZOHAR, Y., LEE, S. Y. K., LEE, W. Y., JIANG, L. & TONG, P. 2002 Subsonic gas flow in a straight and uniform microchannel. *J. Fluid Mech.* **472**, 125–151.